Hydrol. Earth Syst. Sci. Discuss., 9, 6251–6284, 2012
www.hydrol-earth-syst-sci-discuss.net/9/6251/2012/
doi:10.5194/hessd-9-6251-2012

Hydrology and Earth System Sciences Discussions

Integrating MODIS images in a water budget model for dynamic functioning and drought simulation of a Mediterranean forest in Tunisia

H. Chakroun[1], **F. Mouillot**[2], **M. Nouri**[3], **and Z. Nasr**[3]

[1]ENIT, LMHE, BP 37, Tunis 1002, Tunisia
[2]IRD, UMR 5175 – CEFE, Montpellier, France
[3]INRGREF, BP 10, Ariana 2080, Tunisia

Received: 17 April 2012 – Accepted: 29 April 2012 – Published: 16 May 2012

Correspondence to: H. Chakroun (hedia.chakroun@enit.rnu.tn)

Published by Copernicus Publications on behalf of the European Geosciences Union.

Abstract

The use of remote sensing at different spatio-temporal resolutions is being common during the last decades since sensors offer many inputs to water budget estimation. Various water balance models use the LAI as a parameter for accounting water interception, evapotranspiration, runoff and available ground water. The objective of the present work is to improve vegetation stress monitoring at regional scale for a natural forested ecosystem. LAI-MODIS and spatialized vegetation, soil and climatic data have been integrated in a water budget model that simulates evapotranspiration and soil water content at daily step. We first explore LAI-MODIS in the specific context of Mediterranean natural ecosystem. Results showed that despite coarse resolution of LAI-MODIS product (1 km), it was possible to discriminate evergreen and coniferous vegetation and that LAI values are influenced by underlying soil capacity of water holding. The dynamic of vegetation has been integrated into the water budget model by weekly varying LAI-MODIS. Results of simulations were analysed in terms of actual evapotranspoiration, deficit of soil water to field capacity and vegetation stress index based on actual and potential evapotranspiration. Comparing dynamic LAI variation, afforded by MODIS, to a hypothetic constant LAI all over the year correspond to 30 % of fAPAR increase. A sensitivity analysis of simulation outputs to this fAPAR variation reveals that increase of both deficit of soil water to field capacity and stress index are respectively 18 % and 27 %, (in terms of RMSE, these variations are respectively 1258 mm yr^{-1} and 11 days yr^{-1}). These results are consistent with previous studies led at local scale showing that LAI increase is accompanied by stress conditions increase in Mediterranean natural ecosystems. In this study, we also showed that spatial modelisation of drought conditions based on water budget simulations is an adequate tool for quantifying expositions of different species to stress and for analysing most influent factors on ecosystem vulnerability to drought.

HESSD

9, 6251–6284, 2012

1 Introduction

The general context of the present work is to study Mediterranean natural ecosystems vulnerability to drought and climate change by spatial modelling of water budget at regional scale. The lack of such studies over South Mediterranean areas is one of the motivations of this work. In order to contribute in these studies, there is a need to make framework simulations of water budget models by using spatial data at local and regional scales. Such studies attempt to determine critical threshold of available water to ensure the viability of this forested ecosystems in North Africa. Remote sensing (RS) vegetation indices (VI) such as NDVI (Normalized Difference Vegetation Index), EVI (Enhanced Vegetation Index) and derived LAI (Leaf Area Index) have been widely used in surface energy and water balance model (Li et al., 2009; Guerschman et al., 2009; Cleugh et al., 2007; Leuning et al., 2008; Mu et al., 2007; Zhang and Vegehenkel, 2006). According to Edward et al. (2010) in a review study on remote sensing VI estimating evapotranspiration, vegetation indexes are integrated product of LAI, chlorophyll content, leaf angles, fractional cover and canopy architecture over vegetated surfaces (Nagler et al., 2004; Glenn et al., 2007, 2008a, b). All these studies made use of remotely sensed data for water balance estimation and impacts on water storage, long-term catchment and rainfall-runoff models. LAI is an ecosystem functional variable representing the leaf area over a ground area. It is defined as total one-sided leaf area per unit ground surface (Privette et al., 2002). It is an essential parameter for water and carbon budgets, it is measured in situ by comparison of solar energy over and under a canopy to deduce the canopy light interception. The fraction of incident light transmitted through a canopy known as fAPAR (fraction of Absorbed Photosynthetically Active Radiation) is estimated from LAI using a simple Beer's law (Jarvis and Levernez, 1983), known as ($\mathrm{fAPAR} = 1 - \exp^{-k.\mathrm{LAI}}$) where k is extinction coefficient measuring a canopy radiation attenuation. For randomly distributed leaves, this factor is estimated to 0.5 (Sprintsin et al., 2007). Monitoring LAI and fAPAR on regional scale could help in tracking water stress and drought conditions in a given

HESSD
9, 6251–6284, 2012

ecosystem. Indeed, droughts cause a reduction in the vegetation growth rate, which is affected by changes either in the solar interception of the plant or in the light use efficiency (Rossi, 2009). Jamieson et al. (1995) found that a reduction in the intercepted radiation (and therefore in fAPAR) is always a consequence of droughts, both in early or late events. It has been shown in Hoff and Rambal (2003) that LAI greatly affects soil water balance: when LAI increases under constant soil water content and climate conditions, decrease in annual transpiration per unit of LAI is accompanied by an increase in drought stress. LAI and fAPAR are used as satellite derived parameter for calculation of surface photosynthesis, evapotranspiration, soil water retention capacity and annual net primary production (Myneni et al., 2003).

In the last decade, major studies integrating satellite products into water budget monitoring use MODIS (Moderate Resolution Imaging Spectroradiometer) as the satellite sensor system of choice (Edwards et al., 2010). The Terra satellite provides near-daily coverage of the Earth, and MODIS pixels have a resolution of 250 m in the red and near infra red spectral bands and 500 m in the blue band, an improvement over the AVHRR system with 1 km resolution (Huete et al., 2002). The LAI-MODIS product is related to NDVI by the use of visible and near infra red data collected at several view angles and tabular data on land cover type to calculate LAI based on a radiation transfer model (Myneni et al., 2002). As mentioned in Zhang et al. (2006), the general use of MODIS-LAI in hydrological models can be summarized into: the direct estimation of actual evapotranspiration (AET) and comparison of the MODIS data to surface measurements or model-simulated values (Leuning et al., 2005; Xiao et al., 2005) and estimation of canopy water stress. Using physical or empirical models with RS vegetation provides estimation of spatially distributed data with a reasonable degree of accuracy at regional landscape (Guerschman et al., 2009). In Wagner et al. (2009), LAI-MODIS products have been used to incorporate land surface processes, in particular vegetation dynamics, into hydrological simulation in west African site. It has been shown by Zhou et al. (2004) that MODIS images are useful in identifying potential model structure weakness by validation and data assimilation. Other studies on MODIS potential

HESSD
9, 6251–6284, 2012

on water budget estimation were made by Wang et al. (2007) in semi-arid context in the USA (New Mexico, Arizona, and Texas) where a significant relation was showed between responses of MODIS derived NDVI to soil moisture of the root zone in semi-arid and humid natural ecosystem. In Mediterranean ecosystems, use of MODIS images on a Southern Italian forested area by Calcagno et al. (2007) pointed out generally good evapotranspiration predictions especially when MODIS images are upscaled with higher resolution images (e.g. ASTER).

In the present study, our interest is in using the spatial and temporal vegetation dynamic afforded by LAI-MODIS product in a regional water budget for assessing water stress conditions that could lead to drought periods. In Tunisia, studies concerning water stress are rather made in agriculture areas and at local scale (Lhomme et al., 2009). As far as we know, natural vegetation ecosystems have not been subject to water stress studies. The main objectives of our study consist of: (1) making a framework for satellite data (MODIS-LAI) integration in a distributed water budget model. (2) Despite the coarse spatial resolution of MODIS-LAI (1 km), what kind of improvement could this free product afford to regional water budget estimation and drought monitoring. (3) What is the sensitivity of water budget outputs to vegetation dynamic represented by LAI? Answering these questions constitutes a first step for investigating the potential of global images products into spatial water budget modelling and water stress assessment in dense to open Mediterranean forests. Another objective of this work is also to reveal the spatial potential in pointing and monitoring factors that could accentuate water stress and drought precursors: (4) based on spatial framework tools, could we find most relevant factors affecting vulnerability to water stress?

The plan of the article is as follows: water budget model is presented and the main equations and model adaptation are described; next we present data requirements of the model and the processing of satellite data and other ancillary data. We made an exploration of MODIS data and comparisons with in-situ and cartographic data. The outputs of the model are presented in terms of regionalized actual evapotranspiration

HESSD
9, 6251–6284, 2012

maps, soil water deficit and evolution of a spatialized water stress index over the studied forest during one year of simulations.

2 Water budget model description

2.1 General model components

The water budget model used in this study was suggested by Mouillot et al. (2001) for simulating vegetation dynamics based on fluxes of water and carbon for Mediterranean landscapes (SIERRA: Simulator for meditERRAnean landscapes). The main processes of SIERRA model are based on earlier functional models (Mauchamp et al., 1994). Water availability is determined by the infiltration rate and surface runoff. Soil water is simulated down to a maximum depth of 2 m divided in 3 layers; each of them is characterized by its depth and its volumetric storage (in percentage of stones). Local water storage is determined by combining drainage area and average local slope. The model is spatially explicit dealing with gridded stands of vegetation at a specific resolution. Vegetation is considered according to species composition, their intrinsic LAI and associated wood and leaf biomass, and their relative cover within each of three vegetation layers. The model is driven by daily climate values (precipitation, mean temperature and solar radiation).

2.2 Model framework and process

The general process and equations of water budget model are given in Table 1. Inputs are climate, vegetation maps indicating specie composition and relative cover, soil and topography. Each of these components encompasses a set of spatial or spatial/temporal layers. Vegetation components (species and cover) are extracted from processing digital inventory maps and from weekly LAI-MODIS images. Soil components are derived from existing soil maps combined with sample soil analysis information since texture and structure of soils are relevant in soil-vegetation transfers. Water

HESSD
9, 6251–6284, 2012

availability for vegetation is conditioned by water fluxes between soil, plant, and atmosphere, driven by plant capacity to extract water (root profile, maximum plant water potential for extraction) and soil texture, depth and rock fragment content.

We used a modified version of the SIERRA model. In the initial version, the LAI calculation module was based on self-equilibrated leaf biomass according to vegetation carbon budget. This module was replaced by LAI estimated from MODIS time series as already performed in forced vegetation models (e.g. CASA, Potter et al., 1998). To account for the non linear relationship between soil water content and plant functioning, we used the water retention model developed by Saxton et al. (1986) and Saxton et al. (2006) to estimate soil water potential according to soil water content. The soil water potential has been shown to be closely linked to leaf stomatal conductance that limits plant transpiration (Rambal et al., 2003). In this approach, soil water retention curves are determined by texture and organic matter (OM) and their interactions (Hahn, 1982). Water soil potential between 1500 and 33 KPas is varying in exponential manner with soil moisture. A computational program providing Saxton parameters from texture inputs and organic matter content (OM) inputs is available at http://hydrolab.arsusda.gov/soilwater/Index.htm.

The principal model process equations are summarized in Table 1: soil water content at saturation and at field capacity (SWC_{sat}, SWC_{FC}) are determined by Saxton model; then water at filed capacity is computed by considering depth, rock fragment and "Compound Terrain Index" (CTI) (Eq. 1, Clapp and Hornberger, 1978; Mauchamp et al., 1994). Soil water content is determined by Eq. (2) and corresponding soil potential is computed using Saxton model (Eq. 3). Bare soil evaporation is based on diffusion theory (Ritchie, 1972) considering time needed to evaporate a given water deficit daily (Eq. 4). Potential evapotranspiration is computed by Priestley-Taylor equation (Pirestley and Taylor, 1972, Eq. 5) which is a simplified version of Penmann-Monteith equation (Penmann, 1948; Monteith, 1965), and suitable when applied at large scale for several biomes (Fisher et al., 2005). Plant water holding capacity is a fraction of PET decreasing linearly with water potential ratio between soil water potential ψ_s and the specific

HESSD
9, 6251–6284, 2012

maximum potential for soil extraction (ψ_{max} of plant) as long as ψ_s does not exceed ψ_{max} (Mouillot et al., 2001). This leads to AET calculation (Eq. 6, Feddes et al., 1978). Deficit to field capacity is computed as the difference between field capacity and soil water content of all soil layers (Eq. 8).

Based on previous studies in Mediterranean ecosystems (Running, 1984; Rambal, 1993, 1995; Hoff and Rambal, 2003), it has been shown that intensity of drought stress is evidenced by the increase in the number of days per year when predawn leaf water potential is below the critical value for stomatal closure. We use the expression of a normalized water stress index proposed in the case of wheat crops by Lhomme et al. (2009) varying between 0 (no stress) and 1 (total stress) (Eq. 9). Vegetation water stress per year is computed as the sum of daily stress index and annual soil water deficit is the cumulative daily deficit to field capacity. Theses indices may be used for the diagnosis of the vegetation state of drought within a year or many years of simulations.

3 Study site and data requirements

3.1 Site description and multisource mapped data

Study region known as the Kroumirie forest belongs to the Mediterranean North African forests, it is localised at the extreme North of Tunisia (Fig. 1a). This region represents a transition zone between North Mediterranean temperate climate and the Sahara situated at some 400 km away from the forested study region. The Kroumirie forest is extended on a band of about 20 to 30 km width along the Mediterranean coast and covers 2553 km^2. Region climate is Mediterranean with four seasons where precipitations are concentrated in autumn and winter; spring and summer are dry. The maximum average annual precipitations is 1500 mm at Ain Draham with three months of water deficit, the average precipitation of the Kroumirie region in 700 mm (Nasr et al., 2011). Isohyets show an important gradient in the NE-SO direction. The landscape

HESSD
9, 6251–6284, 2012

of the region is typically forested mountains with homogeneous evergreen deciduous trees (43 %), coniferous trees (8 %) and "maquis" (Mediterranean scrubland vegetation at lower slopes of mountains) and "garrigues" (like "maquis", but poorer vegetation on thin soils). Maquis and garrigues represent 49 % of the study area (Fig. 1b). We acquired vegetation maps of the study region from the Forest General Inventory data (Ministry of Agriculture of Tunisia). This digital product in shape format (1:25 000 scale) has been updated in the year 2000; forest polygons have been plotted from photo-interpretation and plots measurements. These data are in structured vector format and projected in Universal Transverse Mercator (UTM, zone 32) system which is the common reference system in Tunisia UTM). For topographic characterization, we use the Aster GDEM product of relief produced at 30 m resolution with stereoscopy process from ASTER images (http://www.gdem.aster.ersdac.or.jp/). This free product was downloaded, clipped to the study region boundaries and georeferenced in UTM projection (Fig. 1a).

Soil data are acquired from digital maps made at 1:100 000 scale original soil map; this map was used as background for producing a national digital format product called "Agriculture Maps". Pedology evolution in study area is largely influenced by the hydrodynamic influx which is conditioned by the external factors in particular slope and organic matter restitution. We extract from original soil maps relevant soil parameters for our study, namely principal soil texture and soil depth (Fig. 1c) and stone contents or fragment rocks. Within each soil polygons considered as homogeneous regarding soil texture, we computed rock fragment content as a function of both soil depth, stone fragment and locally modified by the compound terrain index (Eq. 1) to account for topographical effect on soil accumulation. These data afforded on nominal scales have been improved by laboratory analysis so that we derived quantitative values of texture, organic matter (OM), depth and stone % for each soil class. Water retention potential was calculated from Saxton model (Eq. 3, Fig. 1f).

Daily meteorological observations have been spatially interpolated on a daily basis using automated ordinary kriging, and accounting for altitudinal effects on temperature

HESSD
9, 6251–6284, 2012

and precipitation (Lavoir et al., 2011). Climate data required in Priestley-Taylor PET are daily temperatures, precipitations and net radiation. We acquired measured mean temperatures T and P from four stations in the study region (Beja, Ain Draham, Jendouba, Tabarka) from the "Resource Water Department" (DGRE, Ministry of Agriculture). Regionalisation of meteorological data required the integration of elevation gradient, and derived parameters (slope and aspect). The ASTER-GDEM validated previously by comparison to a stereoscopic DEM in a sub-region of the study area, was processed to derive these two parameters. We used simulated data of global radiation R_g provided at 50 km resolution by ARPEGE General Circulation MODEL (Meteo-France) and we derived approximated net radiation. For T values, the elevation gradient was integrated using the Aster-GDEM elevations ($T_z = T_0 - 0.0066z$; where T_0 is the ground temperature and z is the elevation, Ninyerola et al., 2000). All processed and structured data in both vector and raster formats were integrated into a coherent spatial database for further processing.

3.2 Time-series MODIS data analysis

MODIS images covering North Africa are available since 2002 on the website (http://reverb.echo.nasa.gov/). These 1 km-resolution images correspond to an 8-day composite LAI products (MOD15A2). We also used MOD13Q1 product at a 16-day temporal resolution and 250 m spatial resolution representing NDVI (Normalized Difference Vegetation Index). The tiles covering North Africa region were clipped to the extent of Tunisia. The images were rectified to geographic projection by the use of MODIS reprojection tool. Next, we make a conversion from Geographic projection to Universal Transverse Mercator (UTM, zone 32N). Figure 1b shows a generic LAI image. Compared to vegetation map (Fig. 1c), it is clear that LAI values are higher for evergreen forest (cork and eucalyptus) rather than coniferous (pines). Quality control of the time-series images leads to applying smoothing process to replace some data by the adjacent ones regarding the abrupt variation of LAI values within few days. We compare LAI-MODIS values to in-situ measured values in the study site conducted in 2006 and 2007 over

HESSD
9, 6251–6284, 2012

30 cork oak plots (Ennajah, 2010); these LAI values did not exceed 2.02 $m^2 m^{-2}$. Furthermore, in 2010 LAI measured in the study region reaches 2.8 $m^2 m^{-2}$ (unpublished data). Exploration of weekly LAI-MODIS data shows values widely exceeding these in situ ones; LAI-MODIS reaches more than 6 $m^2 m^{-2}$ especially for high density covers (NDVI > 0.7) (Fig. 2). Values of LAI-MODIS are very high and do not reflect common values measured in south Mediterranean forested areas. This overestimation was also reported by Kanniah et al. (2009) where MODIS-LAI were compared to flux tower in Australia (but it was not that important, about 1 to 20 % overestimation); and in south France (unpublished results). It is important in further processing to correct this overestimation. As a first approximation, we make saturation of LAI values to a maximum of 2.5 $m^2 m^{-2}$.

We made profiles over time to investigate LAI variation for the different vegetation and soil classes described earlier. A profile shows mean values of reference map cells, aggregated by classes and summarized into average values and graphed simultaneously over the sequence of the time-series LAI images. The reference map cells used in this analysis are both forest classes and combination of forest/soil maps. Profiles examination of weekly LAI variation in 2003 for each vegetation class shows two facts (Fig. 3a). First, a seasonal variability of LAI values is observed due to the presence of important herbaceous layer in winter (wet season). This effect was reported in similar studies (e.g. Zhang and Vegehenkel, 2006; Fensholt et al., 2004). Second, there is a clear discrimination of evergreen and coniferous vegetation. Highest values of LAI all over the year are observed with dense evergreen areas. For both species, this discrimination is less important in wet seasons because of the presence of important herbaceous strata.

MODIS-LAI has also been explored regarding soil characteristics. We cross forest and soil data maps by making extraction of forest classes overlaying different soil depths and water holding capacity. For this analysis, we consider only dense forest (both evergreen and coniferous) combined with soil layers (Fig. 3b). Profiles analysis reveal higher LAI values are associated to dense vegetation on medium-depth

HESSD
9, 6251–6284, 2012

compared to shallow soils. We already observed that deep soils are not frequent in the study region; this is why they are not involved in this profile comparison. Besides, higher LAI values are observed for dense vegetation overlaying medium-tension capacity soils compared to high-tension capacity ones. Low-tension soils are not present within region covered by dense forest concerned by this analysis; they are rather covered by "maquis" and "garrigues". Thus, the dynamic of LAI values over a year reveals a difference as we discriminate dense forest on deep/shallow soil and on low/medium tension soil. In this latter case, discrimination was more important. Vegetation response to sensor reported in terms of weekly LAI is influenced by underlying soils capacity of water holding (depth and tension). Similar results have been reported by Wang et al. (2007) who found correlations between NDVI-MODIS and root-zone soil moisture in semi-arid and humid regions. From previous analysis, we can argue that time- series LAI reflect both vegetation and underlying soil holding capacity and, therefore, it can be a useful input in Mediterranean forested ecosystems in water budget models to represent the variability of vegetation state that induces various response in evapotranspiration and soil water storage.

4 Results

Data collected have been spatialized and integrated into a common spatial database. Water budget simulations have been achieved by SIERRA model; input maps resolution were resized to LAI-MODIS 1 km resolution. The other spatial layers were downscaled by averaging data within 1 km cells. Simulations are made at a daily step to account for daily climatic data whereas LAI data is varying each week. Model outputs are daily maps of actual evapotranspiration, soil water content, soil deficit relative to field capacity and stress index.

HESSD
9, 6251–6284, 2012

4.1 Model outputs analysis

We made simulations for one year (2003). Results show that average AET over the study region is 300 mm yr^{-1} with an important standard deviation of 51.5 mm yr^{-1}; AET average calculated for each vegetation class in 2003 are summarized in Table 2. These simulation results are very close to measured sap flow transpiration equal to 308 mm yr^{-1} in cork oak plot in Ain Snoussi site localized in the study zone (Nasr et al., 2009). Spatial mapping of each AET class is illustrated in Fig. 4. We calculate the ratio (AET/P) between annual AET and mean annual precipitation interpolated from mean annual isohyets. This ratio ranges from 0.10 to 0.42 in the study area with an average ratio of 0.27 and a standard deviation of 0.05. Mean daily deficit of soil to field capacity (DFC) is 57 mm day^{-1} with 7 mm day^{-1} standard deviation. Stress index is expressed in terms of days where STR is maximum and reaches 150 days in 2003 for most stressed areas. Spatialization of water budget outputs allows the elaboration of vulnerability maps to stress and to drought at a regional scale. These outputs help observing and comparing trends at regional scale as well as explaining the most influent factors that could potentially aggravate drought process.

4.2 Sensitivity analysis of water balance to vegetation

Integrating weekly LAI-MODIS into water budget model allows a dynamic following of vegetation during the year. A sensitivity analysis was performed to assess the effect of dynamic vegetation represented by LAI-MODIS time series integrated into gridded water budget model. For this purpose, we compare model outputs from two simulations: in the first one LAI is varying each week (LAI_DYN or fAPAR_DYN) and in the second one we considered a constant LAI along the year (LAI_CONS or fAPAR_CONS). We chose 8 sites, characterized in Table 3, to represent variation of model outputs for cork oak dense vegetation localized at different climatic, physiographic and soil conditions. Examples of outputs daily variation over the year of simulation are showed in Fig. 5 for highest and lowest precipitation points (P_{ID6} = 1544 mm; P_{ID7} = 870 mm). Analysis

HESSD
9, 6251–6284, 2012

were first made on a yearly basis showing that LAI dynamic variation along the year influences DFC and STR rather than annual AET (Table 3). This is explained by the fact that AET is higher for dynamic LAI in the first half of summer, and is lower in the second half due to the beginning of stress caused by a cumulative lack of water that is manifested by stomatal closure. The beginning of this period is manifested by a lack of soil water content and corresponds to stress index growth. This index summation over the year gives the total stress days (a and b on ID7 STR graphic in Fig. 5); the number of days where AET_DYN is inferior to AET_CONS is also illustrated in Fig. 5 (c on ID7 STR graphic in Fig. 5) and calculated for each ID test point (NDAYS in Table 3).

We based our comparison of the two simulation scenarios on relative variation and root mean square error (RMSE) computation. Relative variation between afAPAR and model outputs (AET, DFC, STR) have been calculated for each point during dry period as (Δ = (DYN – CONS)/CONS) where DYN and CONS refer respectively to output values with dynamic and constant LAI over the year. Results are summarized in Table 4 showing that for an average Δ(fAPAR) of about 30 % during the year (observed for all test points), Δ(AET) is 1 %, Δ(DFC) is 18 %, and Δ(STR) is 27 % (these variations represent mean values for 8 points). We note that STR relative variation increases with annual precipitation from 20 % to 40 % for a quasi constant fAPAR relative variation of 30 %. These variations computed in terms of RMSE ($RMSE^2 = \Sigma(DYN - CONS)^2/365$) between outputs from simulations with dynamic and constant LAI are summarized in Table 4. First RMSE was determined as the comparison of dynamic-scenario outputs to constant-scenario outputs giving an average daily RMSE. We next report this daily values to the number of days where stress is more important for dynamic-LAI scenario than constant-LAI one (NDAYS in Table 3). Difference between the two scenarios was expressed in terms of RMSE as a reduction of AET by 35 mm, an increase in soil water deficit of 1258 mm and a growth of stress by 11 days (average values over the 8 points).

To summarize, we note that integrating dynamic vegetation by weekly LAI-MODIS images into the water budget model has an important effect on soil water content

HESSD
9, 6251–6284, 2012

estimation and on stress period length. We have showed that dynamic LAI-MODIS integration into water budget model revealed that LAI increase is accompanied by STR increase. This is consistent with studies stipulating that LAI greatly affects site water balance in Mediterranean natural ecosystems (Running, 1984; Rambal, 1993, 1995; Hoff and Rambal, 2003). In these studies, it has been shown that when LAI increases under constant SWC and climate conditions, the decrease in annual transpiration per unit of LAI is accompanied by an increase of drought stress.

4.3 Spatial analysis of drought conditions

Water stress modelled by the spatial water budget model is an important indicator of vulnerability to drought at regional scale. We can take advantage of possibilities of spatial analysis to explain occurrence and most influent factors on vegetation water stress vulnerability. By combining spatial layers of vegetation with annual stress index map, we can assess vulnerability of most important species class to water stress. Evergreen trees (essentially cork oak, and other oaks) cover 48 % of the study area, whereas coniferous are covering 11.2 %. Spatial analysis of occurrence of class stress over these two vegetation classes show that evergreen are less exposed to stress: 59 % of coniferous and 46 % of evergreen (cork and other deciduous) experience more than 3 months of stress (Table 5).

To explain vulnerability to stress, we combine stress map with climatic (annual precipitation and AET/P ratio), soil parameters (soil depth and tension) and relief (slope and CTI). Analysis is conducted by exploring the area of each stress class within each factor class. Results are reported in Table 6 and Fig. 6. Highest stressed areas increase as annual precipitation decreases; the trend is more pronounced with AET/P ratio where more than 93 % of highly stressed areas are within ratio greater than 0.25. For soil factor, 80 % of least stressed areas correspond to low-tension soils; occurrence of most stressed areas increases from 33 to 53 % for low-depth soils (<40 cm) and decreases from 67 to 47 % for soils depth over 40 cm. Topographic effect on stress is not manifested by slope, it is rather clear by combined runoff-slope factor.

HESSD
9, 6251–6284, 2012

5 Discussion and further works

The study develops a general framework for integrating satellite vegetation dynamic into a spatial water budget model. For this purpose, we make use of an existing model developed in a similar context of our study region (South France). Relevant modifications on this original model concerned a best description of soil which is a determinant factor in limited water resource area like forested sites in Northern Tunisia. We also integrate temporal variation of LAI by considering weekly LAI-MODIS product over the study region. Simulations have been made at 1 km resolution. We begin by an exploration of the LAI-MODIS in the special case of South Mediterranean forested ecosystems characterized by its heterogeneity. Despite the coarse resolution of this product, we showed that LAI-MODIS discriminate evergreen and coniferous vegetation and that highest values of LAI all over the year are observed with dense evergreen areas. We also find that vegetation response to sensor reported in terms of weekly LAI is influenced by underlying soils capacity of water holding capacity namely depth and tension. Thus integrating LAI-MODIS into water budget modelisation or any other models involving the vegetation dynamic (such as carbon assimilation, net photosynthesis and water use efficiency) could improve results of simulation. Despite these encouraging results, we find that LAI-MODIS are overestimated compared to measured LAI in the study site. For an efficient use of this product, we recommend to make corrections for these values by saturating the values to the maximum measured, but this could hide the dynamic vegetation. An alternative solution is to calibrate LAI-MODIS by other sources of satellite data with in-situ LAI. The potential of MODIS sensor in such studies is not restricted to LAI products since reflectances measured in middle infra red wavelength (1200–2000 nm) are sensitive to water content of the vegetation. Many moisture vegetation indexes have been proposed (e.g. Fensholt and Sandholt, 2003; Guershman et al., 2009). Comparing simulated stress indexes levels with satellite derived moisture indexes could be an interesting way for validating simulations based on mechanistic models of water process as is the case in this study.

HESSD
9, 6251–6284, 2012

Sensitivity analysis of model outputs to the dynamic of vegetation brought by LAI-MODIS confirms previous results from other studies conducted in similar ecosystem at local scale; these studies showed that increase of LAI is accompanied by increase of drought conditions. We make an attempt to quantify this fact by computing variation of model outputs induced by a variation of LAI (and fAPAR) over a year. Results show that for a relative variation of fAPAR equal to 30 %, stress index increases from 20 to 40 % with annual precipitation increasing from 700 to 1400 mm. We also find that if we consider a constant LAI over a year of simulation, we underestimate DFC by 18 % and STR by 27 %. These variations correspond to RMSE annual values reduction of about 35 mm for AET, an increase in soil water deficit RMSE of 1258 mm and a growth of stress RMSE by 11 days. This sensitivity analysis is consistent with studies stipulating that LAI greatly affects site water balance in Mediterranean natural ecosystems.

Regional modelisation of drought conditions through stress index derived from water budget modelisation allows the assessment of most influent factors on vegetation stress. Spatial analysis reveal that 60 % of coniferous and 45 % of evergreen (cork and other deciduous) experience more than 3 months of stress during the simulation year. Ratio AET/P is highly correlated to stress index since more than 93 % of highly stressed areas are within ratio greater than 0.25. Soil holding capacity of water represented by soil tension and depth explain also the high stressed area: 80 % of least stressed areas correspond to low-tension soils and 53 % of most stressed areas have low-depth soils ($\delta_s < 40$ cm).

Finally, in the past two years, the study region of Kroumirie is beginning to be quipped by one ground measuring station of evapotranspiration (Nasr et al., 2009) and 35 temperature stations to account for microclimate, and fuel water status studies across the gradient. This will allow combination of measured values, satellite data and simulated variables for enhancing our understanding of ecohydrological process in this ecosystem which is known as one of the most vulnerable to climate change (IPCC, 2007). Combination of multisource data into the spatial database elaborated and integrated to

HESSD
9, 6251–6284, 2012

water budget models is an appropriate tool for making simulations of future climate and the potential drought conditions that could be reached by this ecosystem in the future.

Acknowledgements. This study was supported by the CORUS 2 (Coopération pour la Recherche Universitaire et Scientifique, Ministry of Foreign Affairs of France). Authors wish to thank the Ministry of Agriculture and Water Resources of Tunisia for providing digital maps and climatic data, and NASA Earth Science Enterprise for providing free MODIS images on the web.

References

Calcagno, G., Mendicino, G., Monacelli, G., Senatore, A., and Versace, P.: Distributed estimation of actual evapotranspiration through remote sensing techniques, in: Methods and Tools for Drought Analysis and Management, edited by: Rossi, G., Teodoro, V., and Brunelle, B., Springer, 125–147, 2007.

Chen, J. M., Chen, X., Ju, W., and Geng, X.: Distribution hydrological model for mapping evapotranspiration using remote sensing inputs, J. Hydrol., 305, 15–39, 2005.

Clapp, R. B. and Hornberger, G. M.: Empirical equations for some soil hydraulic properties, Water Resour. Res., 14, 601–604, 1978.

Cleugh, H. A., Leuning, R., Mu, Q., and Runnig, S. X.: Regional evaporation estimates from flux flower tower and MODIS satellite data, Remote Sens. Environ., 106, 285–304, 2007.

Edward, P. G., Nagler, P. L., and Huete, A. R.: Vegetation index methods for estimating evapotranspiration by remote sensing, Surv. Geophys., 31, 531–555, 2010.

Ennajah, A.: Croissance et productivité des forêts de chêne liège "*Quercus suber* L." en Tunisie, Vulnérabilité aux changements climatiques, Ph.D. Thesis, Faculty of Sciences of Tunis, 241 pp., 2010.

Feddes, R. A., Kowalik, P. J., and Zaradny, H.: Simlations of Field Water Use and Crop Yield, Wagenigen, 1978.

Fensholt, R. and Sandholt, I.: Derivation of a shortwave infrared stress index from MODIS near- and shortwave infrared data in semi arid environment, Remote Sens. Environ., 87, 111–121, 2003.

HESSD

9, 6251–6284, 2012

Fensholt, R., Sandholt, I., and Rasmussen, M. S.: Evaluation of MODIS LAI, fAPAR and the relation between fAPAR and NDVI in a semi-arid enviornement using in situ measurements, Remote Sens. Environ., 91, 490–507, 2004.

Fisher, J. B., DeBiase, T. A., Qi, Y., Xu, M., and Goldstein, A. H.: Evapotranspiration models compared on a sierra nevada forest ecosystem, Environ. Modell. Softw., 20, 783–796, 2005.

Glenn, E. P., Huete, A. R., Nagler, P. L., Hirschboek, K., and Brown, P.: Integrating remote sensing and ground methods to estimate evapotranspiration, Crit. Rev. Plant Sci., 26, 139–168, 2007.

Glenn, E. P., Huete, A. R., Nagler, P. L., and Nelson, S. G.: Relationship between remotely-sensed vegetation indices, canopy attributes and plant physiological processes: what vegetation indices can and cannot tell us about the landscape, Sensors, 8, 2136–2160, 2008a.

Glenn, E. P., Morino, K., Didan, K., Jordan, F., Carroll, K. C., Nagler, P. L., Hultine, K., Sheader, L., and Waugh, J.: Scaling sap flux measurements of grazed and ungrazed shrub communities with fine and coarseresolution remote sensing, Ecohydrology, 1, 316–329, 2008b.

Guerschman, J. P., Van Dijk, A. I. J. M., Mattersdorf, G., Beringer, J., Hutley, L. B., Leuning, R., Pinpunic, R. C., and Sherman, B. S.: Scaling of potential evapotranspiration with MODIS data reproduces flux observations and catchment water balance observations across Australia, J. Hydrol., 369, 107–119, 2009.

Hahn, C. T.: Statistical methods in hydrology, Iowa State University Press, 1982.

Hoff, C. and Rambal, S.: An examination of the interaction between climate, soil and leaf area index in a *Quecus ilex* ecosystem, Ann. For. Sci., 60, 153–161, 2003.

Huete, A., Didan, K., Miura, T., Rodriquez, E., Gao, X., and Ferreira, L.: Overview of the radiometric and biophysical performance of the MODIS vegetation indices, Remote Sens. Environ. 83, 195–213, 2002.

IPCC: Working Group III contribution to the Intergovernmental Panel on Climate Change, Fourth Assessment Report Climate Change 2007: Mitigation of Climate Change, 2007.

Jamieson, P. D., Martin, R. J., Francis, G. S., and Wilson, D. R.: Drought effects on biomass production and radiation-use efficiency in barley fields, Crops Res., 43, 77–86, 1995.

Jarvis, P. G. and Leverenz, J. W.: Productivity of Temperate Deciduous and Evergreen Forests, Springer, New York, 1983.

HESSD

9, 6251–6284, 2012

Kanniah, K. D., Beringer, J., Hutley, L., Tapper, N., and Zhu, X.: Evaluation of collections 4 and 5 of the MODIS gross primary productivity product and algorithm improvement at a tropical savanna site in Northern Australia, Remote Sens. Environ., 113, 1808–1822, 2009.
Lavoir, A. V., Duffet, C., Mouillo, F., Rambal, S., Ratte, J. P., Schnitzler, J. P., and Staudt, M.: Scaling-up leaf monoterpene emissions from a water limited *Quercus ilex* woodland, Atmos. Environ., 45, 2888–2897, 2011.
Leuning, R., Cleugh, H. A., Zegelin, S. J., and Hughes, D.: Carbon and water fluxes over a temperate Eucalyptus forest and a tropical wet/dry savanna in Australia: measurements and comparison with MODIS remote sensing estimates, Agr. Forest Meteorol., 129, 151–173, 2005.
Leuning, R., Zegelin, S. J., Jones, K., Keith, H., and Hughes, D.: A mass-balance technique for measuring CO_2 fluxes in nocturnal drainage flows beneath a forest canopy, Agr. Forest Meteorol., 148, 1777–1797, 2008.
Lhomme, J. P., Mougou, R., and Mansour, M.: Potential impact of climate change on durum wheat cropping in Tunisia, Climatic Change, 96, 549–564, 2009.
Li, H., Zhang, Y., Chiew, F. H. S., and Xu, S.: Predicting runoff in ungauged catchments by using Xinanjiang model with MODIS leaf area index, J. Hydrol., 370, 155–162, 2009.
Mauchamp, A., Rambal, S., and Lepart, J.: Simulating the dynamics of vegetation mosaics: a spatialized functional model, Ecol. Modell., 71, 107–130, 1994.
Monteith, J. L.: Evaporation and environment, Symp. Soc. Expl. Biol., 19, 205–234, 1965.
Mouillot, F., Rambal, S., and Lavorel, S.: A generic process-based simulator for Mediterranean landscapes (SIERRA): design and validation exercices, Forest Ecol. Manage., 147, 75–97, 2001.
Myneni, R., Hoffman, S., Knyazikhim, Y., Privette, J. L., Glassy, J., Tian, Y., Wang, Y., Song, X., Zhang, Y., Smith, G. R., Lotsch, A., Friedl, M., Morisette, J. T., Votava, P., Nemani, R. R., and Running, S. W.: Global products of vegetation leaf area index and fraction absorbed PAR from year one of MODIS data, Remote Sens. Environ., 83, 214–231, 2002.
Myneni, R., Hoffman, S., Knyazikhin, Y., Privette, J., Glassy, J., and Tian, Y.: Global products of vegetation leaf area and fraction absorbed PAR from year one of MODIS data, Remote Sens. Environ., 83, 214–231, 2003.
Mu, Q. M., Zhao, S., and Running, W.: Improvements to a MODIS global terrestrial evapotranspiration algorithm, Remote Sens. Environ., 115, 1781–1800, 2007.

HESSD
9, 6251–6284, 2012

Nagler, P., Glenn, E., Thompson, T., and Huete, A.: Leaf area index and normalized difference vegetation index as predictors of canopy characteristics and light interception by riparian species on the Lower Colorado River, Agr. Forest Meteorol., 116, 103–112, 2004.
Nasr, Z., Zineddine, M., Khaldi, A., Woo, S. Y., Nouri, M., Khorchani, A., Stiti, B., and Rejeb, M. N.: Seasonal variations of evapotranspiration and net carbon assimilation in a cork oak forest North Tunisia, 6th Meeting on Integrated Protection of *Quercus* spp. Forests, Tempio Pausania, Italy, 2009.
Nasr, Z., Woo, S. Y., Zineddine, M., Khaldi, A., and Rejeb, M. N.: Sap flow estimates of *Quercus suber* according to climatic conditions in north Tunisia, Afr. J. Agric. Res., 6, 4705–4710, 2011.
Ninyerola, M., Pons, X., and Roure, J. M.: Methodological approach of climatological modelling of air temperature and precipitation through GIS techniques, Int. J. Climatol., 20, 1823–1841, 2000.
Penman, H. L.: Natural evaporation from open water, bare soil and grass, P. R. Soc. London, 193, 120–145, 1948.
Priestley, C. H. B. and Taylor, R. J.: On the assessment of surface heat flux and evaporation using large scale parameters, Mon. Weather Rev., 100, 81–92, 1972.
Potter, C. S., Davidson, E. A., Klooster, S. A., Nepstad, D. C., De Negreiros, G. H., and Brooks, V.: Regional application of an ecosystem production model for studies of biogeochemistry in Brasilian Amazonian, Glob. Change Biol., 4, 315–333, 1998.
Privette, J. L., Myneni, R. B., Knyazikhin, Y., Mukelabai, M., Roberts, G., Tian, Y., Wang, Y., and Leblanc, S. G.: Early, spatial and temporal validation of MODIS LAI product in the Southern Africa Kalahari, Remote Sens. Environ., 83, 232–243, 2002.
Rambal, S.: The differential role of mechanisms for drought resistance in a Mediterranean evergreen shrub: a simulation approach, Plant Cell Environ., 16, 35–44, 1993.
Rambal, S.: From daily transpiration to seasonal water balance: an optimal use of water? in: Time Scale of Biological Response to Water Constraints, edited by: Roy, J., Aronson, J., and di Castri, F., SPB Academic Publ., 37–51, 1995.
Rambal, S., Ourcival, J. M., Joffre, R., Mouillot, F., Nouvellon, Y., Reichstein, M., and Rocheteau, A.: Drought controls over conductance and assimilation of a Mediterranean evergreen ecosystem: scaling from leaf to canopy, Glob. Change Biol., 9, 1813–1824, 2003.
Ritchie, J. T.: Model for predicting evaporation from row crop with incomplete cover, Water Resour. Res., 8, 1204–1212, 1972.

HESSD
9, 6251–6284, 2012

Rossi, S.: Remote Sensing for drought monitoring, 1st joint DMCSEE – JRC Workshop on Drought Monitoring, Ljubljana, 21–25 September, 2009.
Running, S. W.: Microclimate control of forest productivity: analysis by computer simulation of annual photosynthesis/transpiration balance in different environment, Agr. Forest Meteorol., 3, 267–288, 1984.
Saxton, K. E. and Rowls, W. J.: Soil water characteristic estimates by texture and organic matter for hydrologic solutions, Soil Sci. Soc. Am. J., 70, 1569–1578, 2006.
Saxton, K. E., Rawls, W. J., Romberger, J. S., and Papendick, R. I.: Estimating generalized soil water characteristics from texture, T. ASAE, 50, 1031–1035, 1986.
Sprintsin, M., Karnieli, A., Berliner, P., Rotenberg, E., Yakir, D., and Cohen, S.: The effect of spatial resolution on the accuracy of leaf area index estimation for a forest planted in the desert transition zone, Remote Sens. Environ., 109, 416–428, 2007.
Wagner, S., Kunstmann, H., Bárdossy, A., and Colditz, R. R.: Water balance estimation of a poorly gauged catchment in West Africa using dynamically downscaled meteorological fields and remote sensing information, Phys. Chem. Earth, 34, 225–235, 2009.
Wang, X., Xie, H., Guan, H., and Zhou, X.: Different responses of MODIS-derived NDVI to root-zone soil moisture in semi-arid and humid regions, J. Hydrol., 340, 12–24, 2007.
Xiao, X. M., Zhang, Q. Y., Hollinger, D., Aber, J., and Moore, B.: Modeling gross primary production of an evergreen needle leaf forest using MODIS and climate data, Ecol. Appl., 15, 954–969, 2005.
Zhang, Y. and Wegehenkel, M.: Integration of MODIS data into a simple model for the spatial distributed simulation of soil water content and evapotranspioration, Remote Sens. Environ., 104, 393–408, 2006.
Zhou, S. Q., Liang, X., Chen, J., and Gong, P.: An assessment of the VIC-3L hydrological model for the Yangtze River basin based on remote sensing: a case study of the Baohe River basin, Can. J. Remote Sens., 30, 840–853, 2004.

HESSD
9, 6251–6284, 2012

Table 1. Equations of principal process in water budget SIERRA model.

Equations		Parameters
$FC_i = SWC_{FC}(1-\eta_i)$	(1)	DAILY CLIMATE DATA:
where		T: Temperature °C
$\eta_1 = \eta_s$		P: Precipitation (mm)
$\eta_2 = \eta_3 = 0.5\left(\frac{120-\delta_s}{120}\right) + 0.25\left(\frac{2-CTI}{2}\right) + 0.25\eta_s$		P_{EFF}: Efficient precipitation (mm)
and		R_n: Net radiation ($J\,cm^{-2}$)
$CTI = \ln\left(\frac{Runoff}{tg(Slope)}\right)$		RELIEF DATA:
		Elevation, Slope, Aspect, Runoff
		Runoff: accumulation of rainfall units per pixel
		based on an elevation image
		CTI: Compound Terrain Index
$SWC_{i,j} = \min[(SWC_{i,j-1} + P_{EFF}), FC_i]$	(2)	SOIL DATA:
where		Texture (%)
$P_{EFF} = P - 0.5LAI$		OM: Organic matter content (%)
		δ_s: soil depth (cm)
		η_s: % of stone
$(\psi_s)_{i,j} = A\left(\frac{SWC_{i,j}}{SWC_{SAT}}\right)^{-B}$	(3)	η_1, η_2, η_3: % of stone of first, second
		and third layer of soil
		A, B: Saxton coefficient
$E_j = G(\sqrt{t_{FICT}+1} - \sqrt{t_{FICT}})(1-e^{-k\,LAI})EV_i$	(4)	SWC_{SAT}: Soil water content at saturation (0 kPas) (mm) (Saxton model)
		SWC_{FC}: Soil Water content at field capacity
$PET = C_{H_2O}\alpha\frac{\Delta}{\Delta+\gamma}R_n$	(5)	(33 kPas) (mm) (Saxton model)
		$SWC_{i,j}$: Soil water content in layer i at day j (mm)
$AET_j = PET_j\left(1-e^{-(k\,LAI)}\right)\left(1-\frac{(\psi_s)_{i,j}}{\psi_{max}}\right)$	(6)	FC: Water content at field capacity (mm)
		EV_i: Soil evaporation of different layers:
		90 % (0–20 cm), 7.5 % (20–100 cm), 2.5 % (100–120 cm)
$(SWC_{i,j})_{final} = (SWC_{i,j})_{initial} - E_j - AET_j$	(7)	E_j: Evaporation bare soil at day j (mm)
		G: Ritchie Evaporation parameter (5 kPas°C^{-1})
$DFC_j = \sum_{i=1}^{3}(FC_i - SWC_{i,j})$	(8)	t_{FICT}: Time needed to evaporate DFC (s)
		ψ_s: Soil potential (KPas)
		DFC: Deficit to field capacity (mm)
$STR_j = 1 - \frac{AET_j}{PET_j}$	(9)	VEGETATION DATA:
		LAI: Leaf Area Index ($m^2\,m^{-2}$)
		ψ_{max}: Maximum extraction potential of each specie (KPas)
		k: Extinction coefficient of evaporation (mm^{-1})
		C_{H_2O}: Water vapour heat (245 $J\,cm^{-2}$ evaporates 1 mm of water)
		α: Coefficient of Priestley-Taylor (= 1.26)
		γ: Psychrometric constant (= 0.66 kPas°C^{-1})
		Δ: Gradient of saturated vapour pressure (kPas°C^{-1})
		PET: Potential evapotranspiration (mm)
		AET: Actual evapotranspiration (mm)

HESSD
9, 6251–6284, 2012

Table 2. Annual simulated AET of each class vegetation in Kroumirie in 2003.

Vegetation class	Average AET ($mm\,yr^{-1}$)
Evergreen dense	315
Evergreen sparse	318
Coniferous dense	296
Coniferous sparse	311
Maquis and garrigues with cork	283
Maquis and garrigues with cork	217

HESSD
9, 6251–6284, 2012

Table 3. Simulation outputs for points selected within the study region.

ID	ELEV (m)	P_2003 (mm)	SCENARIO LAI_DYN AET ($mm\,yr^{-1}$)	SCENARIO LAI_DYN DFC ($mm\,day^{-1}$)	SCENARIO LAI_DYN STR ($days\,yr^{-1}$)	SCENARIO LAI_CONS AET ($mm\,yr^{-1}$)	SCENARIO LAI_CONS DFC ($mm\,day^{-1}$)	SCENARIO LAI_CONS STR ($days\,yr^{-1}$)	NDAYS
ID1	313	1000	365	100	146	359	87	121	53
ID2	407	1153	359	82	149	358	69	119	79
ID3	286	991	305	80	152	311	71	129	63
ID4	243	916	352	97	151	342	86	129	47
ID5	571	1449	382	82	127	390	65	89	81
ID6	690	1544	375	75	112	389	61	84	64
ID7	157	870	390	123	150	389	109	124	63
ID8	503	1402	306	43	127	312	34	92	72

HESSD
9, 6251–6284, 2012

Table 4. Relative variation and RMSE of simulation outputs based on dynamic-LAI and constant-LAI vegetation.

ID	ΔfAPAR	ΔAET	ΔDFC	ΔSTR	RMSE AET ($mm\,day^{-1}$)	RMSE DFC ($mm\,day^{-1}$)	RMSE STR ($mm\,day^{-1}$)	RMSE AET ($mm\,yr^{-1}$)	RMSE DFC ($mm\,yr^{-1}$)	RMSE STR ($mm\,yr^{-1}$)
ID1	33 %	2 %	14 %	21 %	0.61	19	0.16	32	1018	9
ID2	32 %	0 %	19 %	26 %	0.51	20	0.17	40	1598	13
ID3	28 %	−2 %	13 %	18 %	0.45	14	0.14	29	917	9
ID4	31 %	3 %	12 %	18 %	0.59	17	0.15	28	789	7
ID5	29 %	−2 %	26 %	44 %	0.60	25	0.21	48	2066	17
ID6	31 %	−3 %	23 %	33 %	0.57	22	0.15	36	1391	10
ID7	29 %	0 %	12 %	21 %	0.56	20	0.14	35	1245	9
ID8	33 %	−2 %	27 %	37 %	0.42	14	0.19	30	1038	14
MEAN	31 %	−1 %	18 %	27 %	0.54	18.87	0.16	35	1258	11
STDEV	1 %	2 %	6 %	10 %	0.07	3.79	0.02	7	419	3

HESSD
9, 6251–6284, 2012

Table 5. Percentage of simulated stressed areas in Kroumirie region in 2003.

Number of vegetation stress months	Coniferous	Evergreen
1	15 %	14 %
2	29 %	33 %
3	41 %	54 %
4	69 %	81 %
5	100 %	100 %

HESSD
9, 6251–6284, 2012

Table 6. Results of spatial analysis of vegetation stress periods within different factors classes.

Factor	Class factor	Low STR < 2 months yr^{-1}	Medium STR 2–3 months yr^{-1}	High STR 3–4 months yr^{-1}	Extreme STR 4–5 months yr^{-1}
Precipitation	700–1000 mm	65 %	62 %	77 %	74 %
	1000–1400 mm	35 %	38 %	23 %	26 %
AET/P	0.1–0.25	69 %	55 %	7 %	0 %
	0.25–0.55	31 %	45 %	93 %	100 %
Soil depth	0–40 cm	33 %	41 %	45 %	53 %
	> 40 cm	67 %	59 %	55 %	47 %
Soil tension	B (Saxton) < 7.7	79 %	82 %	77 %	67 %
	B (Saxton) > 7.7	21 %	18 %	23 %	33 %
Slope	Slope < 10 %	51 %	47 %	51 %	57 %
	Slope > 10 %	49 %	53 %	49 %	43 %
CTI	1–7	72 %	74 %	70 %	60 %
	7–11	28 %	26 %	30 %	40 %

HESSD
9, 6251–6284, 2012

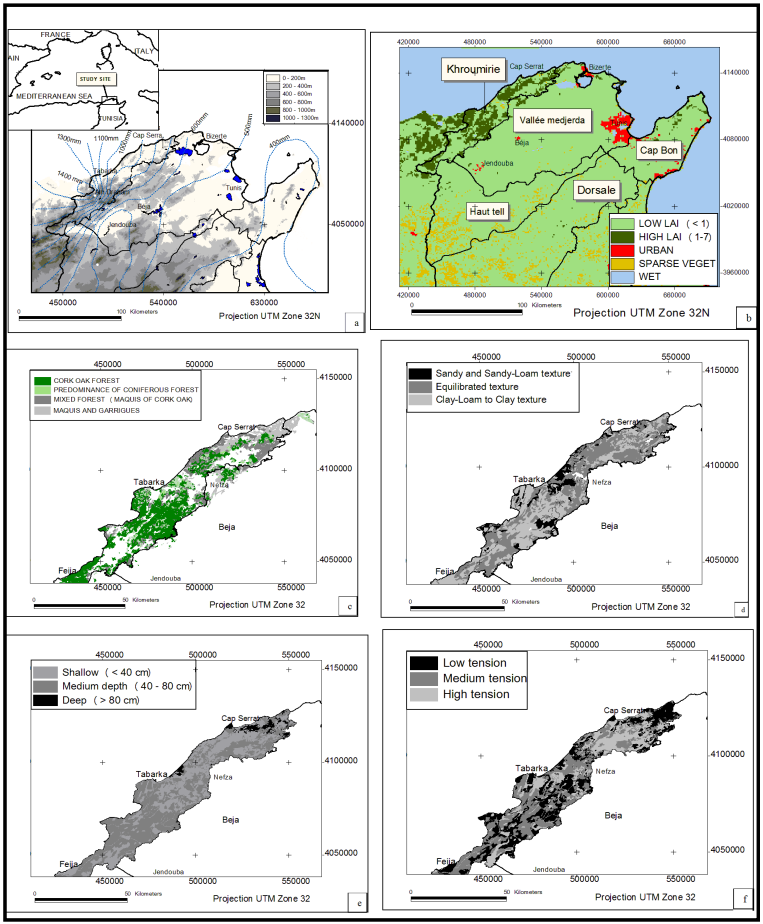

Fig. 1. Study site localization and multisource spatial data: **(a)** ASTER-GDEM and isohyets, **(b)** generic LAI-MODIS, **(c)** forest map, **(d)** soil texture, **(e)** soil depth and **(f)** soil tension.

HESSD
9, 6251–6284, 2012

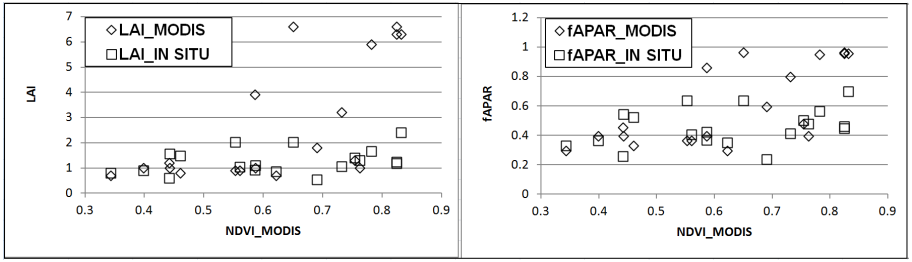

Fig. 2. Comparison of LAI-MODIS and fAPAR to in situ LAI in the Kroumirie region.

HESSD
9, 6251–6284, 2012

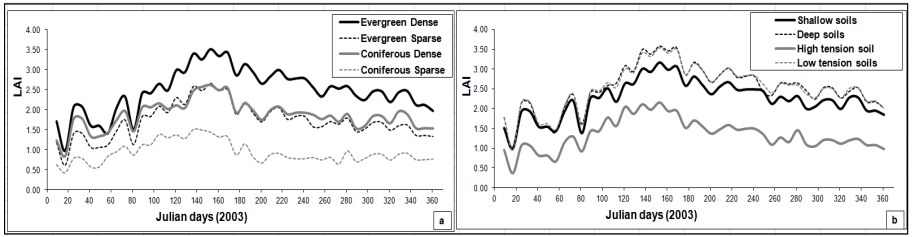

Fig. 3. LAI-MODIS variation within **(a)** vegetation and **(b)** vegetation/soil properties.

HESSD
9, 6251–6284, 2012

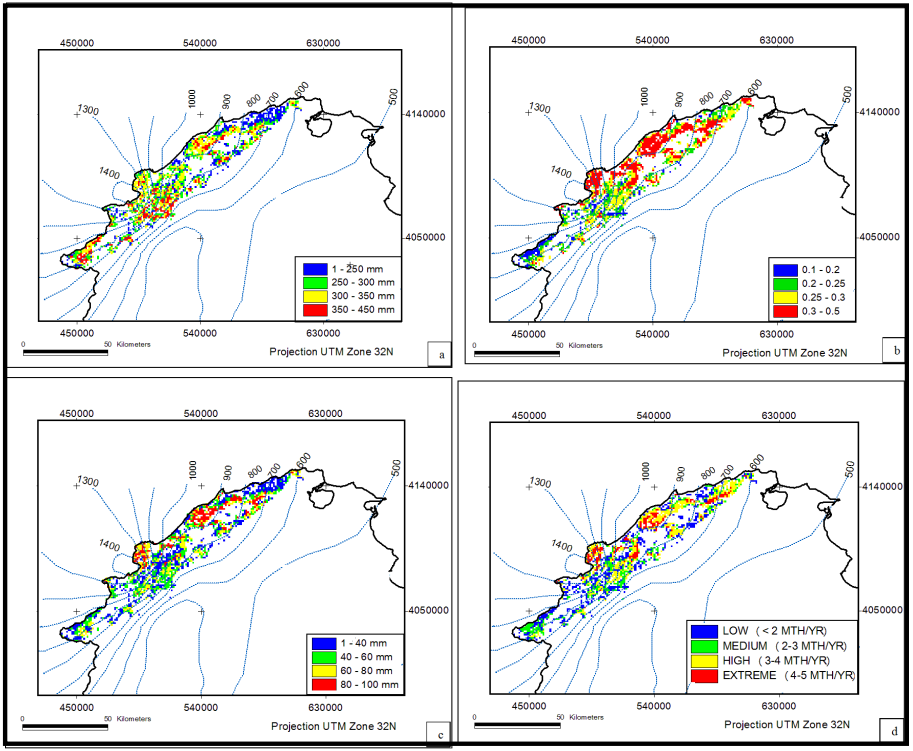

Fig. 4. Spatial distribution of water budget simulation outputs **(a)**: AET (mm yr^{-1}) **(b)**: AET/*P*, **(c)**: Average DFC (mm day^{-1}) and **(d)**: STR (months yr^{-1}).

HESSD
9, 6251–6284, 2012

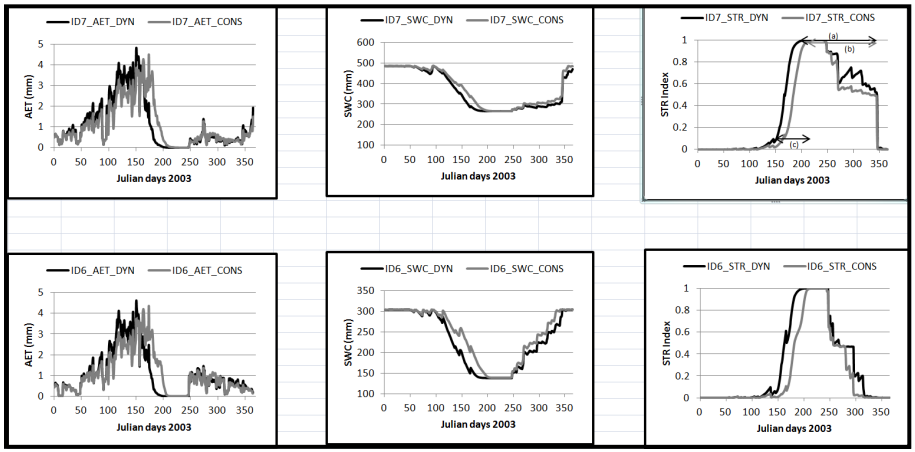

Fig. 5. Profiles of daily outputs simulation (AET, SWC and STR) for highest precipitation point (P_ID_6 = 1544 mm) and least precipitation point (P_ID_7 = 870 mm). Results correspond to weekly LAI-MODIS (DYN) and constant LAI (CONS).

HESSD
9, 6251–6284, 2012

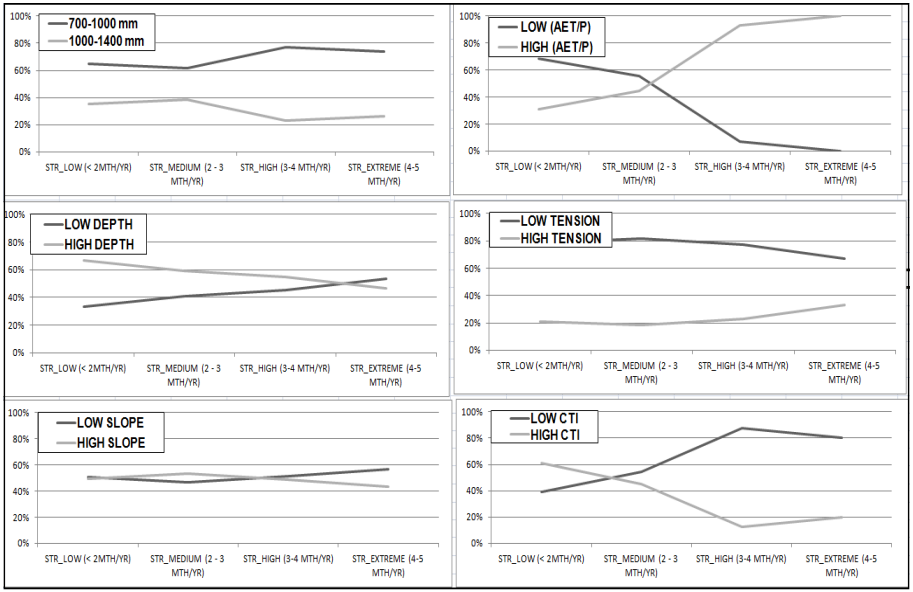

Fig. 6. Variation of stress index period with climate, soil and relief in the study region.

HESSD
9, 6251–6284, 2012